Distributed Target Localization and Encirclement with a Multi-Robot System

Antonio Franchi * **Paolo Stegagno** * **Maurizio Di Rocco** **
Giuseppe Oriolo *

* *Dipartimento di Informatica e Sistemistica, Università di Roma La Sapienza, via Ariosto 25, 00185 Roma, Italy (e-mail: franchi,stegagno,oriolo@dis.uniroma1.it).*
** *Dipartimento di Informatica e Automazione, Università Roma Tre, via della Vasca Navale 79, 00146 Roma, Italy (e-mail: dirocco@dia.uniroma3.it)*

Abstract: This paper presents a control scheme for localizing and encircling a target using a multi-robot system. The task is achieved in a distributed way, in that each robot only uses local information gathered by on-board relative-position sensors assumed to be noisy, anisotropic, and unable to detect the identity of the measured object. Communication between the robots is provided by limited-range transceivers. Experimental results with stationary and moving targets support the theoretical analysis.

Keywords: Multi-robot systems, distributed control, mutual localization, encirclement.

1. INTRODUCTION

This paper addresses the problem of localizing and encircling a target by means of a multi-robot system, a task which appealed to the robotics literature in view of the large number of potential applications, among which we mention *observation* (retrieve and merge data about an object from different viewpoints), *escorting* (protect a member of the system from unfriendly agents) and *entrapment* (prevent the motion of an alien object).

Several control techniques have been recently proposed to achieve encirclement or similar formation control objectives. Leonard and Fiorelli (2001) make use of virtual points to deform the shape of the formation and take care of collision avoidance. Gazi and Passino (2002) analyze the performance of a swarm approaching a goal and its cohesion in the presence of attractive and repulsive profiles. Moreau (2005) presents a control law whose convergence is based on the topology of the communication graph. Lin et al. (2005) consider a fixed-topology algorithm based on the concept of $\alpha-$*stability*, while consensus results are applied to formation control by Ren (2007). In (Sepulchre et al., 2007) a group of unicycles is steered in a regular formation around a common point. Strictly related to this approach is the work presented in (Moshtagh et al., 2009) where a centralized vision system is used for the experimentation. In (Ceccarelli et al., 2008) a controller for encirclement with nonholonomic robots with directional sensors is designed using a Lyapunov approach. Noisy measurements and distributed estimation have been considered only in recent works such as (Yang et al., 2008), where the passivity property of the system is used, and (Sepulchre et al., 2008), where a controller based on the quality of the estimate is analyzed. A different approach is used in (Antonelli et al., 2008), where a global vision system provides the configuration of each robot to a centralized controller. A loosely related problem is pursuit-evasion, addressed, among the others, in (Bopardikar et al., 2009).

In our solution, target localization and encirclement are achieved in a *distributed* way, i.e., each robot acts only on the basis of the local information gathered by on-board transceivers and sensors, both limited in range. We assume that each robot measures the relative position of other robots and of the target with a single sensor which is noisy and anisotropic. Moreover, the sensor is unable to provide the identity of the measured object or any information to identify the target among the measured robots. We exploit the mutual localization method introduced in our previous work (Franchi et al., 2009) to localize the robots and the target, overcoming the geometric limitations of our minimal sensor model, i.e., limited range, blind spots, and anisotropy. To our knowledge, this is the first work that includes experiments on a set-up in which localization is not provided by a centralized module, such as a vision system that uses tags to discriminate the robots. This shows that our approach is viable in a real unstructured context in which each robot needs to estimate the quantities needed by the control law on the basis of local information only.

The paper is organized as follows. In Sec. 2, the encirclement problem is formally defined. In Sec. 3 we describe the proposed system architecture, while in Sec. 4 its control module is thoroughly analyzed. Conditions for effective task execution are derived in Sec. 5, while Sec. 6 presents some experimental results. Finally, Sec. 7 hints at on-going and future work.

2. PROBLEM FORMULATION

Consider a group of identical mobile robots with unicycle kinematics and a target, all moving on the plane. The target may be an inanimate object, a robot, or even a living

agent. The task assigned to the robots is to *encircle* the target, i.e., move around it in a regular circular formation, also called a *splay state* formation (Sepulchre et al., 2008). The target is assumed to be stationary for the sake of analysis, but we will experimentally show in Sect. 6 that 'slow' movements may be accommodated. No a priori information is available about the cardinality of the group, the initial configuration the robots, and the position of the target. In addition, the task must be realized on the basis of local sensory information only.

Clearly, the encirclement task requires each robot of the group to be able to localize the target as well as the other robots. We may distinguish between two cases, depending on whether the appearance of the target is *identical* to or *different* from that of the robots. In the first case, the robots and the target may be detected by a single sensory device, whereas two separate detectors (a robot detector and a target detector) must be used in the second case. In this paper, we shall consider in detail the first case; however, the proposed technique can be trivially extended to the second.

A target that appears to be identical to the robots may be an unfriendly agent in disguise that must be made inoffensive, or actually one of the robots that must be guarded or escorted by the others. An unfriendly target does not communicate with the other robots (*non-cooperating target*), while communication with a friendly target is obviously possible (*cooperating target*).

We assume that each robot is equipped with:

(1) A *robot detector*, a sensor device that measures the relative position (not the orientation) of other robots and of the target w.r.t. the detector, provided that they fall in a perception set D_p that is rigidly attached to it. The shape of D_p is arbitrary, and in particular it may contain blind zones. The relative position measures provided by the robot detector are *anonymous*, i.e., they do not convey the specific identity of the detected robot (hence, the target is detected as a robot).
(2) A *communication module* that can send/receive data to/from any other robot contained in a communication set D_c such that $D_p \subseteq D_c$.

Under the above assumptions, it may happen that one robot can detect another, but not vice versa; in other words, the robot *detection graph* is directed (and includes the target as a *sink*). However, if one robot can detect another it can also communicate with it; the *communication graph* is therefore undirected and contains the detection graph, with the exception of the target and its in-arcs. In the following, two robots that can communicate with each other are simply called *neighbors*.

3. SYSTEM ARCHITECTURE

The encirclement system installed on each robot, shown in Fig. 1, consists of two main modules. The *mutual localizer* is in charge of computing the configuration of the robot in a reference frame centered at the target. This information is passed to the *encirclement controller*, that generates a reference trajectory for the robot and the feedback control inputs that guarantee its tracking.

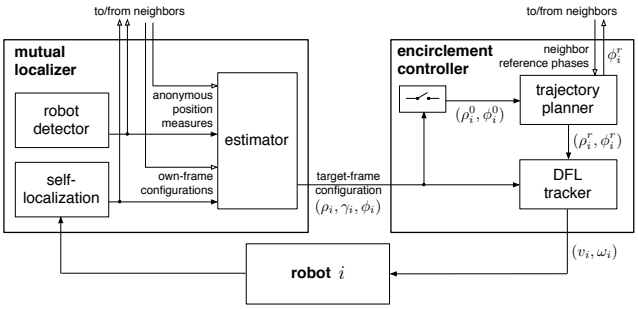

Fig. 1. The structure of the encirclement system that runs on the i-th robot.

The mutual localization module implements the method proposed by Franchi et al. (2009), to which the reader is referred for a detailed description. The inputs to this component are (1) the anonymous relative position measures (which include the target, if this is contained in D_p) coming from the robot detector (2) an estimate of the configuration of the robot in its own frame, computed by any self-localization (position tracking) algorithm (3) the same information (i.e., anonymous relative position measures and robot configuration in its own fixed frame) obtained via communication from each neighbor. A multiple registration algorithm followed by a multi-EKF are used to process these data and compute an accurate estimate of the configuration of each robot in a common fixed frame. While a cooperating target is directly identified and localized with this procedure, it is interesting to note that a non-cooperating target can still be singled out by the mutual localization module as the only 'robot-like' object that does not communicate its data. From the mutual localization results, each robot can directly derive an estimate of its configuration (position and orientation) with respect to a *common* target-centered frame.

The encirclement control module generates the control inputs to the robot using the target-centered configuration of the robot computed by the mutual localizer as well as information coming from the neighbor robots. The structure of this module is discussed in detail in the following section.

4. ENCIRCLEMENT CONTROLLER

In view of the encirclement objective, it is convenient to express the configuration of the generic i-th robot in polar coordinates with respect to a reference frame centered at the target, as in Fig. 2. In particular, these coordinates are the distance ρ_i of the unicycle wheel center from the origin, the angle γ_i that the sagittal (forward) axis of the robot forms with the line joining the unicycle wheel center to the origin, and the angle ϕ_i between the same line and the x axis. In the following, ϕ_i is also called *phase* of the robot. The kinematic model of the unicycle is then written as (Aicardi et al., 1995)

$$\begin{aligned} \dot{\rho}_i &= -v_i \cos\gamma_i \\ \dot{\gamma}_i &= (\sin\gamma_i)/\rho_i - \omega_i \\ \dot{\phi}_i &= v_i(\sin\gamma_i)/\rho_i, \end{aligned}$$

where v_i and ω_i are respectively the driving and steering velocity inputs.

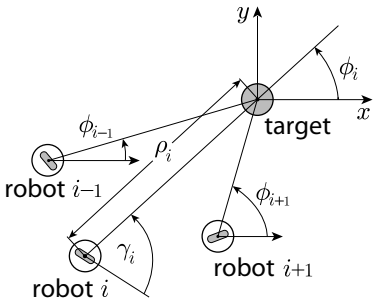

Fig. 2. Polar coordinates for the i-th robot and the cyclic ordering defined by phases.

It is assumed that the robot index i refers to the cyclic counterclockwise ordering of the robots defined by their increasing phase angles (see Fig. 2). For the i-th robot, denote by $\bar{\phi}_i$ the mean between the phases of the successor (robot $i+1$) and the predecessor (robot $i-1$) of the robot. Correct execution of the encirclement task requires that

$$\lim_{t\to\infty} \rho_i(t) = R \qquad \lim_{t\to\infty} \phi_i(t) = \bar{\phi}_i(t) \qquad \lim_{t\to\infty} \dot{\phi}_i(t) = \Omega \quad \forall i, \tag{1}$$

where R and Ω are respectively the encirclement radius and angular speed, which must be the same for all robots.

The entrapment control module (see Fig. 1) works as follows. The initial configuration $(\rho_i^0, \gamma_i^0, \phi_i^0)$, provided by the mutual localization module [1] is used to plan a reference trajectory for the robot. In particular, such trajectory is specified by an exosystem that assigns reference evolutions ρ_i^r, ϕ_i^r to the coordinates ρ_i, ϕ_i. In fact, it is easy to verify that these two are *flat* outputs (Fliess et al., 1995) for the unicycle in polar coordinates, i.e., once an evolution is assigned to them it is possible to compute algebraically the corresponding evolution γ_i^r of the remaining variable γ_i as well as the reference inputs v_i^r, ω_i^r. The reference outputs ρ_i^r, ϕ_i^r are fed to a feedback controller based on Dynamic Feedback Linearization (DFL), that generates the control inputs v_i, ω_i so as to guarantee global exponential tracking of the reference trajectory (Oriolo et al., 2002). It should be noted that ρ_i^r, ϕ_i^r are initialized at ρ_i^0, γ_i^0, so that the transient is extremely fast. During its operation, the DFL tracker uses the current estimate of the target-frame robot configuration $(\rho_i, \gamma_i, \phi_i)$ computed by the mutual localization module.

In the following, we consider three slightly different versions of the basic encirclement task entailed by (1), and give the appropriate form of the trajectory planner (exosystem). In all versions, the encirclement radius R is assigned in advance. The reference radius $\rho_i^r(t)$ is therefore always generated by

$$\dot{\rho}_i^r = K_\rho(R - \rho_i^r) \qquad \rho_i^r(0) = \rho_i^0, \tag{2}$$

where K_ρ is a positive gain. As a consequence, $\rho_i^r(t)$ exponentially converges to R for any initial condition. Note that $\rho_i^r(t)$ does not depend on the reference radius of any other robot.

[1] This assumes that the configuration estimate is immediately reliable. In practice, it may be necessary to perform a preliminary motion of the multi-robot system aimed at improving the accuracy of the estimate. To this end, the anti-symmetry control law proposed in (Franchi et al., 2010) may be used.

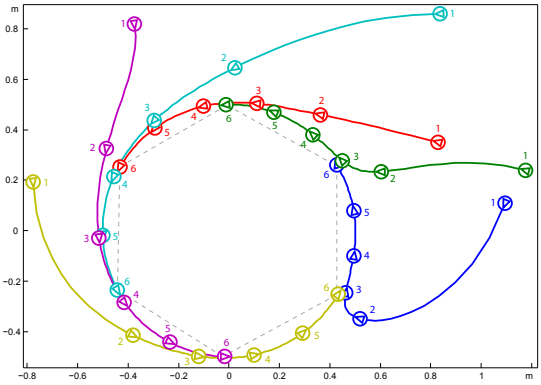

Fig. 3. Reference trajectories corresponding to the flow of (2),(3) for a generic initial configuration of a 6-robot system, with a target located at the origin. The configuration of each reference robot along its trajectory is explicitly shown at six equispaced time instants, identified by $1, \ldots, 6$.

The three versions of the encirclement task differ on the procedure used by the robots to agree on the common value of the angular speed Ω in (1). They are analyzed in detail below.

Encirclement – Version 1. In the first version, the angular speed Ω is also specified in advance. The reference phase $\phi_i^r(t)$ for the i-th robot is generated by

$$\dot{\phi}_i^r = \Omega + K_\phi(\bar{\phi}_i^r - \phi_i^r) \qquad \phi_i^r(0) = \phi_i^0, \tag{3}$$

where K_ϕ is a positive gain and $\bar{\phi}_i^r$ is the mean between the reference phases of the predecessor and the successor (in accordance with the counterclockwise cyclical ordering of the reference phases). We have the following result (the proofs of all the propositions are in the Appendix).

Proposition 1. The flow of (2),(3) yields exponential convergence of ρ_i^r to R, of ϕ_i^r to $\bar{\phi}_i^r$, and of $\dot{\phi}_i^r$ to Ω, for any assigned R, Ω and any initial ρ_i^0, ϕ_i^0.

An example of reference robot trajectories corresponding to the flow of (2),(3) is shown in Fig. 3. The robots approach the circle in such a way that the 'insertion points' are almost uniformly spaced, and actually achieve the required formation very quickly.

Encirclement – Version 2. In the second version, the robots are assigned an *escape window* s, i.e., the time interval in which a point on the circle remains unvisited at the steady state corresponding to the asymptotic conditions (1). Being $s = 2\pi/n\Omega$, where n is the number of robots, the robots can in principle easily compute the required value of Ω as $\Omega = 2\pi/ns$; however, since n is not known a priori, an estimate $\hat{n}$ of this number is required.

Assume that each robot instantaneously computes its own estimate as $\hat{n}_i = 2\pi/\Delta_i^r$, where $2\Delta_i^r$ is the reference phase difference between the successor and the predecessor. The required angular speed for the robot is then computed as $\Omega_i = 2\pi/\hat{n}_i s = \Delta_i^r/s$. Using this expression for Ω in (3) we obtain the following exosystem for the reference phase:

$$\dot{\phi}_i^r = \Delta_i^r/s + K_\phi(\bar{\phi}_i^r - \phi_i^r) \qquad \phi_i^r(0) = \phi_i^0. \tag{4}$$

Proposition 2. The flow of (2),(4) yields exponential convergence of ρ_i^r to R, of ϕ_i^r to $\bar{\phi}_i^r$, and of $\dot{\phi}_i^r$ to $2\pi/ns$, for any assigned R, s and any initial ρ_i^0, ϕ_i^0.

Encirclement – Version 3. In the third version, only the radius R is assigned, and the robots must autonomously agree on a common value of the angular speed Ω. The reference phase exosystem for the i-th robot is

$$\dot{\Omega}_i^r = K_\Omega(\bar{\phi}_i^r - \phi_i^r) \qquad \Omega_i^r(0) = 0 \qquad (5)$$

$$\dot{\phi}_i^r = \Omega_i^r + K_\phi(\bar{\phi}_i^r - \phi_i^r) + \xi_i \qquad \phi_i^r(0) = \phi_i^0 \qquad (6)$$

where ξ_i is a costant forcing term. Denote by $\bar{\xi}$ the average of the forcing terms ξ_i over the multi-robot system.

Proposition 3. The flow of (2), (5–6) yields exponential convergence of ρ_i^r to R, of ϕ_i^r to $\bar{\phi}_i^r$, and of $\dot{\phi}_i^r$ to $\bar{\xi}$, for any assigned R and any initial ρ_i^0, ϕ_i^0.

An interesting feature of this third scheme is that the common frequency of the phase reference trajectories can be regulated by acting on a single robot; to this end, it is sufficient to let $\xi_i = 0$ for all the robots but one.

To allow the implementation of (3), (4), or (5–6) all the robots must broadcast their current reference phase through the communication system. However, each robot computes its reference trajectory and control inputs autonomously on the basis of local information, i.e., its own configuration and data coming from the neighbors.

5. CONDITIONS FOR TASK ACHIEVEMENT

The proposed method will achieve the encirclement task provided that the robots can localize the target and each other. In this section, we briefly discuss the conditions under which these two requirements are actually satisfied. Recall that the mutual localization module used in our encirclement scheme is effective within weakly connected components (simply called *subnets* in the following) of the robot detection graph, provided that $D_p \subseteq D_c$ and multi-hop communication is used (Franchi et al., 2009).

The first condition may be derived from the analysis of the desired steady state of the system, in which the n robots are uniformly distributed along a circle of radius R. In this formation, the whole detection graph must be weakly connected, i.e., a single subnet must exist. In view of the circle topology, this property is certainly guaranteed if each robot can detect the target and the successor robot with respect to the cyclic phase ordering (that is actually the predecessor if Ω is positive). For example, this is true if D_p is a frontal circular sector with central angle at least $\pi + \epsilon$ wide, with ϵ any positive number, and radius at least $\max\{R, 2R\sin\pi/n\}$.

The second condition is instead obtained considering the beginning of the encirclement task. To localize the target at $t = 0$, each subnet of the detection graph must contain at least one robot that detects the target. From that moment on, all the robots will get closer to the target in view of the reference evolution (2) for ρ, and therefore target detection is guaranteed throughout the task (this is easy to show if D_p has the shape discussed above). In particular, all the subnets will merge into a single connected component that includes the whole graph.

Note that the first condition (on D_p) concerns the robot detector, whereas the second (on the detection graph at $t = 0$) restricts the admissible initial arrangements of the robots with respect to the target. Taken together, they are a *sufficient* condition for task achievement — less demanding requirements may be enforced (in particular, on the shape of D_p) but their efficacy would be more difficult to prove.

6. EXPERIMENTS

The proposed localization/encirclement scheme has been experimentally validated using Khepera III robots. Each robot is equipped with a wi-fi card and a Hukuyo URG-04LX laser sensor. The latter has an angular range of 240° and a linear range artificially limited to 2 m. The robot detector is a simple feature extraction algorithm that searches the laser scan for the indentations made by the vertical cardboard squares mounted on each robot (in the blind zone of the range finder). Since each square can give indentations of the laser scan that are $1 \div 12$ cm wide depending on the relative orientation between the measuring and the measured robot, the detector cannot distinguish among robots, the target and obstacles whose size is in the same range. Simple odometry is used as self-localization. The localization/encirclement scheme has been implemented using the MIP architecture [2], which provides a multi-tasking estimation/control framework, a realistic simulation environment and allows direct porting for execution on real robots.

A complete experiment is summarized in Fig. 4. Here, we are considering version 1 of the encirclement task, and hence (2–3) as a trajectory planner, with $R = 0.5$ m and $\Omega = 0.06$ rad/s. One of the robots is used as a stationary, cooperating target. At the start (snapshot 1), only three robots are active. At $t_1 = 200$ s, with the three robots rotating around the target in a regular formation, another robot is added (dashed circle in snapshot 2); the robots then achieve a square formation (snapshot 3). At $t_2 = 310$ s one of the robots is manually displaced (snapshot 4) and then released, but the robots recover the square formation (not shown), thanks to the mutual localizer which quickly recovers the large odometry error. At $t_3 = 490$ s one of the robot is switched off and removed. The three remaining robots rearrange themselves in a regular formation (snapshot 5). Finally, at $t_4 = 600$ s another robot is removed and the formation becomes a 1 m wide dipole. The evolution of the experiment is also illustrated by Fig. 5, that shows the plots of the distances between consecutive robots, the distances between each robot and the target, and the robot angular speeds. The fact that during each phase the correct regular formation is promptly reached shows the reactivity of the proposed encirclement scheme.

We have also run experiments with moving targets, obtaining satisfactory results as long as the speed of the target remains at least one order of magnitude smaller than that of the robots. One such experiment is shown in Fig. 6. Video clips of the experiments are available at http://www.dis.uniroma1.it/labrob/research/encirclement.html.

[2] http://www.dis.uniroma1.it/∼labrob/software/MIP/index.html

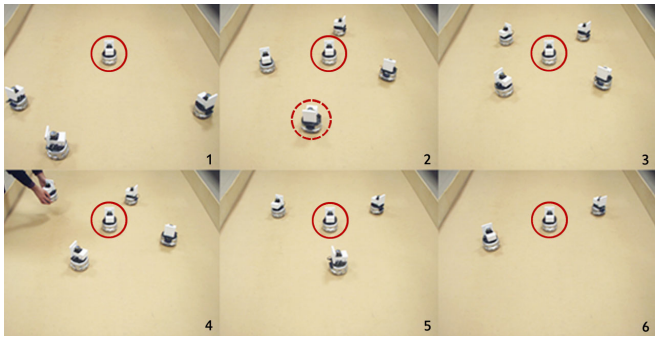

Fig. 4. Encirclement of a stationary target (solid red circle).

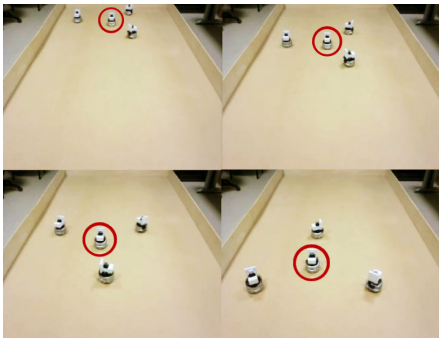

Fig. 6. Encirclement of a moving target (solid red circle).

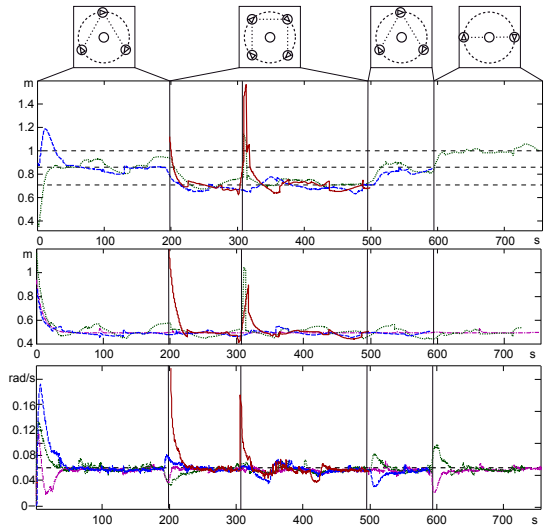

Fig. 5. Plots for the previous experiment: distances between consecutive robots (top), distances between each robot and the target (center), angular speeds of the robots (bottom).

7. CONCLUSIONS

We have presented a distributed control method for encircling a target by means of a multi-robot system. The proposed scheme integrates a mutual localization module based on the developments in (Franchi et al., 2009). The theoretical proof of its effectiveness is supported by extensive experimental results.

Future work will be aimed at:

- proving that the reference trajectories never meet, so as to provide grounds for identifying a collision avoidance condition for robots of finite size;
- performing a theoretical analysys of a trajectory generation scheme based on *continuous replanning*, in which the actual robot coordinates (estimated through the mutual localization module) are used in place of their reference value (we already implemented such a variant with encouraging results);
- integrating a *consensus* mechanism among the robots on the results of the mutual localization, and especially the configuration of the target.

REFERENCES

Aicardi, M., Casalino, G., Bicchi, A., and Balestrino, A. (1995). Closed loop steering of unicycle like vehicles via Lyapunov techniques. *IEEE Robotics & Automation Magazine*, 2(1), 27–35.

Antonelli, G., Arrichiello, F., and Chiaverini, S. (2008). The entrapment/escorting mission: An experimental study using a multirobot system. *IEEE Robotics & Automation Magazine*, 15(1), 22–29.

Bopardikar, S.D., Bullo, F., and Hespanha, J.P. (2009). A cooperative Homicidal Chauffeur game. *Automatica*, 45(7), 1771–1777.

Ceccarelli, N., Di Marco, M., Garulli, A., and Giannitrapani, A. (2008). Collective circular motion of multi-vehicle systems. *Automatica*, 44(12), 3025–3035.

Fliess, M., Lévine, J., Martin, P., and Rouchon, P. (1995). Flatness and defect of nonlinear systems: Introductory theory and examples. *International Journal of Control*, 61(6), 1327–1361.

Franchi, A., Oriolo, G., and Stegagno, P. (2009). Mutual localization in a multi-robot system with anonymous relative position measures. In *2009 IEEE/RSJ Int. Conf. on Intelligent Robots and Systems*, 3974–3980. St. Louis, MO.

Franchi, A., Oriolo, G., and Stegagno, P. (2010). On the solvability of the mutual localization problem with anonymous position measures. In *2010 IEEE Int. Conf. on Robotics and Automation*, 3193–3199. Anchorage, AK.

Gazi, V. and Passino, K.M. (2002). Stability analysis of social foraging swarms: combined effects of attractant/repellent profiles. In *41th IEEE Conf. on Decision and Control*, 2848–2853. Las Vegas, NV.

Leonard, N.E. and Fiorelli, E. (2001). Virtual leaders, artificial potentials and coordinated control of groups. In *40th IEEE Conf. on Decision and Control*, 2968–2973. Orlando, FL.

Lin, Z., Francis, B., and Maggiore, M. (2005). Necessary and sufficient graphical conditions for formation control of unicycles. *IEEE Trans. on Automatic Control*, 50(1), 121–127.

Moreau, L. (2005). Stability of multiagent systems with time-dependent communication links. *IEEE Trans. on Automatic Control*, 50(2), 169–182.

Moshtagh, N., Michael, N., Jadbabaie, A., and Daniilidis, K. (2009). Vision-based, distributed control laws for motion coordination of nonholonomic robots. *IEEE Trans. on Robotics*, 25(4), 851–860.

Oriolo, G., De Luca, A., and Vendittelli, M. (2002). WMR control via dynamic feedback linearization: Design, implementation, and experimental validation. *IEEE Trans. on Control Systems Technology*, 10(6), 835–852.

Ren, W. (2007). Consensus strategies for cooperative control of vehicle formations. *IET Control Theory & Applications*, 1(2), 505–512.

Sepulchre, R., Paley, D.A., and Leonard, N.E. (2007). Stabilization of planar collective motion: All-to-all communication. *IEEE Trans. on Automatic Control*, 52(5), 811–824.

Sepulchre, R., Paley, D.A., and Leonard, N.E. (2008). Stabilization of planar collective motion with limited communication. *IEEE Trans. on Automatic Control*, 53(3), 706–719.

Yang, P., Freeman, R.A., and Lynch, K.M. (2008). Multi-agent coordination by decentralized estimation and control. *IEEE Trans. on Automatic Control*, 53(11), 2480–2496.

Appendix A. PROOFS

We index the robots accordingly to the ordering of the initial reference phases, and we use the following notations:

$$\mathbf{1} = (1 \cdots 1)^T, \quad \boldsymbol{b} = (-\pi\ 0 \cdots 0\ \ \pi)^T, \quad \boldsymbol{g} = (\pi\ 0 \cdots 0\ \pi)^T,$$
$$\boldsymbol{\phi}^r = (\phi_1^r\ \cdots\ \phi_n^r)^T, \quad \bar{\boldsymbol{\phi}}^r = \boldsymbol{C}\boldsymbol{\phi}^r + \boldsymbol{b}, \quad \boldsymbol{\Delta}^r = \boldsymbol{D}\boldsymbol{\phi}^r + \boldsymbol{g},$$
$$\boldsymbol{\Omega}^r = (\Omega_1^r\ \cdots\ \Omega_n^r)^T, \quad \boldsymbol{\xi} = (\xi_1\ \cdots\ \xi_n)^T,$$

where $\boldsymbol{C}$ and $\boldsymbol{D}$ are the *circulant matrices* with first rows $(0\ 1/2\ 0\ \cdots\ 0\ 1/2)$, and $(0\ -1/2\ 0\ \cdots\ 0\ 1/2)$ respectively. The presence of $\boldsymbol{b}$ and $\boldsymbol{g}$ in the definition of $\bar{\boldsymbol{\phi}}^r$ and $\boldsymbol{\Delta}^r$ takes into account the fact that

$$\bar{\phi}_1^r = (\phi_2^r + \phi_n^r - 2\pi)/2, \quad \bar{\phi}_n^r = (\phi_1^r + 2\pi + \phi_{n-1}^r)/2,$$
$$\Delta_1^r = (\phi_2^r - \phi_n^r + 2\pi)/2, \quad \Delta_n^r = (\phi_1^r + 2\pi - \phi_{n-1}^r)/2,$$

and allows to encode the topology of S^1 in $\mathbb{R}$. Also, denote by $\boldsymbol{e}_\phi = \bar{\boldsymbol{\phi}}^r - \boldsymbol{\phi}^r = (\boldsymbol{C}-\boldsymbol{I})\boldsymbol{\phi}^r + \boldsymbol{b}$ and $\boldsymbol{e}_\Omega = \boldsymbol{\Omega}^r + \boldsymbol{\xi} - \bar{\xi}\mathbf{1}$ the phase and pulsation error vectors, where $\boldsymbol{I}$ is the identity.

Proof of Proposition 1. Writing (3) for all the robots we obtain

$$\dot{\boldsymbol{\phi}}^r = \Omega\mathbf{1} + K_\phi(\bar{\boldsymbol{\phi}}^r - \boldsymbol{\phi}^r).$$

In order to prove the statement, it is sufficient to show that $\boldsymbol{e}_\phi$ goes to zero. Note that $\mathbf{1}^T(\boldsymbol{C}-\boldsymbol{I}) = (\boldsymbol{C}-\boldsymbol{I})\mathbf{1} = \mathbf{0}$, i.e., $\boldsymbol{C}$ is balanced; $\ker(\boldsymbol{C}-\boldsymbol{I}) = \mathrm{span}\{\mathbf{1}\}$ and the algebraic multiplicity of 0 is 1; all the other eigenvalues are negative, i.e., $\boldsymbol{C}-\boldsymbol{I}$ is negative semidefinite [3]. Writing the error dynamics we obtain

$$\dot{\boldsymbol{e}}_\phi = K_\phi(\boldsymbol{C}-\boldsymbol{I})\boldsymbol{e}_\phi + \Omega(\boldsymbol{C}-\boldsymbol{I})\mathbf{1} = K_\phi(\boldsymbol{C}-\boldsymbol{I})\boldsymbol{e}_\phi.$$

Hence, the error converges to its initial average, which is zero for any initial condition, since

$$\mathbf{1}^T\boldsymbol{e}_\phi(0) = \mathbf{1}^T(\boldsymbol{C}-\boldsymbol{I})\boldsymbol{\phi}^r(0) + \mathbf{1}^T\boldsymbol{b} = \mathbf{0}. \qquad \blacksquare$$

Proof of Proposition 2. Writing (4) for all the robots, and letting $f = 1/s$, we obtain

$$\dot{\boldsymbol{\phi}}^r = f\boldsymbol{\Delta}^r + K_\phi(\bar{\boldsymbol{\phi}}^r - \boldsymbol{\phi}^r).$$

The error dynamics in this case is

$$\dot{\boldsymbol{e}}_\phi = K_\phi(\boldsymbol{C}-\boldsymbol{I})\boldsymbol{e}_\phi + f(\boldsymbol{C}-\boldsymbol{I})(\boldsymbol{D}\boldsymbol{\phi}^r + \boldsymbol{g}).$$

Since $\boldsymbol{C}-\boldsymbol{I}$ and $\boldsymbol{D}$ commute, we have

$$\dot{\boldsymbol{e}}_\phi = (K_\phi(\boldsymbol{C}-\boldsymbol{I}) + f\boldsymbol{D})\boldsymbol{e}_\phi + f((\boldsymbol{C}-\boldsymbol{I})\boldsymbol{g} - \boldsymbol{D}\boldsymbol{b}),$$

and being $(\boldsymbol{C}-\boldsymbol{I})\boldsymbol{g} - \boldsymbol{D}\boldsymbol{b} = \mathbf{0}$ we conclude that

$$\dot{\boldsymbol{e}}_\phi = (K_\phi(\boldsymbol{C}-\boldsymbol{I}) + f\boldsymbol{D})\boldsymbol{e}_\phi.$$

[3] It is the Laplacian of the undirected ring with weights 1/2.

The matrix $K_\phi(\boldsymbol{C}-\boldsymbol{I}) + f\boldsymbol{D}$ has the same properties [4] of $K_\phi(\boldsymbol{C}-\boldsymbol{I})$ which was used to show the convergence of $\boldsymbol{e}_\phi$ to $\mathbf{0}$ in the Proof of Proposition 1. This implies also that $\hat{\phi}_i^r$ converges to $2\pi/n$ and $\dot{\phi}_i^r$ to $2\pi/ns$. $\blacksquare$

For the proof of Proposition 3 we need a preliminary result.

Lemma. Consider a $2n \times 2n$ matrix of the form

$$\boldsymbol{A} = \begin{pmatrix} \mathbf{0} & k_1\boldsymbol{I} \\ \boldsymbol{B} & k_2\boldsymbol{B} \end{pmatrix}$$

where $\mathbf{0}$ is the $n \times n$ null matrix, $\boldsymbol{I}$ is the $n \times n$ identity matrix, $\boldsymbol{B}$ is a $n \times n$ matrix, and k_1, k_2 are non-zero real numbers. For any eigenvalue μ of $\boldsymbol{B}$ associated to the eigenvector $\boldsymbol{u}$, the two roots of $\lambda^2 - k_2\mu\lambda - k_1\mu$, denoted with $\lambda_{1,2}$, are eigenvalues of $\boldsymbol{A}$ associated to the eigenvectors $\left(k_1\boldsymbol{u}^T\ \ \lambda_{1,2}\boldsymbol{u}^T\right)^T$.

Proof. A vector $\left(\boldsymbol{v_1}^T, \boldsymbol{v_2}^T\right)^T$ is an eigenvector of $\boldsymbol{A}$ associated to λ if

$$k_1\boldsymbol{v_2} = \lambda\boldsymbol{v_1} \tag{A.1}$$
$$\boldsymbol{B}\boldsymbol{v_1} + k_2\boldsymbol{B}\boldsymbol{v_2} = \lambda\boldsymbol{v_2}. \tag{A.2}$$

Hence, from (A.1), the eigenvectors have the structure $(k_1\boldsymbol{v}\ \ \lambda\boldsymbol{v})$. Letting $\boldsymbol{v} = \boldsymbol{u}$ in this structure, and substituting it into (A.2) we obtain $k_1\mu\boldsymbol{u} + k_2\lambda\mu\boldsymbol{u} = \lambda^2\boldsymbol{u}$, which establishes the Lemma. $\blacksquare$

Proof of Proposition 3. Writing (5),(6) for all the robots we obtain

$$\dot{\boldsymbol{\Omega}}^r = K_\Omega(\bar{\boldsymbol{\phi}}^r - \boldsymbol{\phi}^r), \quad \boldsymbol{\Omega}_d(0) = \mathbf{0} \tag{A.3}$$
$$\dot{\boldsymbol{\phi}}^r = \boldsymbol{\Omega}^r + K_\phi(\bar{\boldsymbol{\phi}}^r - \boldsymbol{\phi}^r) + \boldsymbol{\xi}. \tag{A.4}$$

Let us consider the dynamics of the error $\boldsymbol{e} = (\boldsymbol{e}_\phi^T\ \boldsymbol{e}_\Omega^T)^T$

$$\dot{\boldsymbol{e}} = \begin{pmatrix} K_\Omega\boldsymbol{e}_\phi \\ (\boldsymbol{C}-\boldsymbol{I})(\boldsymbol{\Omega}^r + \boldsymbol{u}) + K_\phi(\boldsymbol{C}-\boldsymbol{I})\boldsymbol{e}_\phi \end{pmatrix} =$$
$$= \begin{pmatrix} \mathbf{0} & K_\Omega\boldsymbol{I} \\ \boldsymbol{C}-\boldsymbol{I} & K_\phi(\boldsymbol{C}-\boldsymbol{I}) \end{pmatrix} \begin{pmatrix} \boldsymbol{e}_\Omega \\ \boldsymbol{e}_\phi \end{pmatrix} = \tilde{\boldsymbol{A}}\boldsymbol{e},$$

where we have made use of the fact that $\bar{\xi} = (1/n)(\mathbf{1}^T\boldsymbol{\xi})$ and $(\boldsymbol{C}-\boldsymbol{I})\mathbf{1} = \mathbf{0}$. Recalling that $\boldsymbol{C}-\boldsymbol{I}$ is balanced, negative semi-definite, and noting that its smallest eigenvalue is -2, and applying the Lemma to $\tilde{\boldsymbol{A}}$ we can conclude that all the real parts of its eigenvalues have the same sign of the eigenvalues of $\boldsymbol{C}-\boldsymbol{I}$ (in fact, they are simply related by a 1/2 factor). Furthermore, the algebraic multiplicity of the eigenvalue 0 of $\tilde{\boldsymbol{A}}$ is 2, and its generalized eigenspace is generated by $\mathrm{span}\{(\mathbf{1}^T\ \mathbf{0}^T)^T, (\mathbf{0}^T\ \mathbf{1}^T)^T\}$. Since, by construction, $\mathbf{1}^T\boldsymbol{e}_\Omega(0) = 0$ and $\mathbf{1}^T\boldsymbol{e}_\phi(0) = 0$, there is no evolution over this unstable eigenspace, which implies that $\boldsymbol{e}$ goes exponentially to zero. $\blacksquare$

Note that Propositions 1, 2, and 3 imply that the reference phases are asymptotically in the same order as the initial reference phases. It can be proved that the same property actually holds along the *whole* duration of the trajectories of (3) and (4); the proof is lengthy and therefore omitted. Presently, this is only a (likely) conjecture for (5–6).

[4] It is the Laplacian of the undirected ring with different weights.